

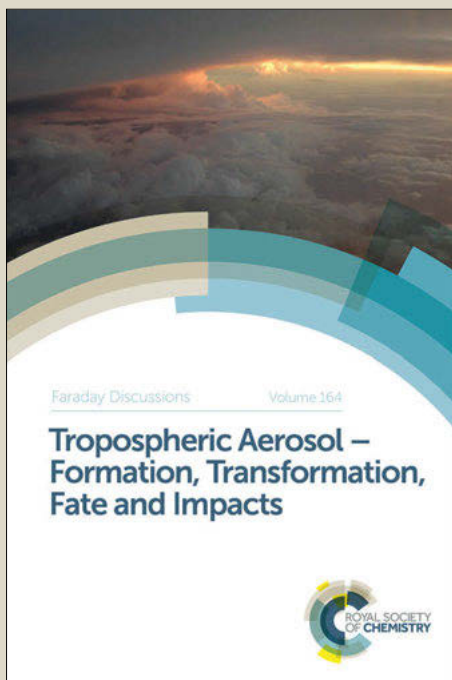
Faraday Discussions

Accepted Manuscript



This manuscript will be presented and discussed at a forthcoming Faraday Discussion meeting. All delegates can contribute to the discussion which will be included in the final volume.

Register now to attend! Full details of all upcoming meetings: <http://rsc.li/fd-upcoming-meetings>



This is an *Accepted Manuscript*, which has been through the Royal Society of Chemistry peer review process and has been accepted for publication.

Accepted Manuscripts are published online shortly after acceptance, before technical editing, formatting and proof reading. Using this free service, authors can make their results available to the community, in citable form, before we publish the edited article. We will replace this *Accepted Manuscript* with the edited and formatted *Advance Article* as soon as it is available.

You can find more information about *Accepted Manuscripts* in the [Information for Authors](#).

Please note that technical editing may introduce minor changes to the text and/or graphics, which may alter content. The journal's standard [Terms & Conditions](#) and the [Ethical guidelines](#) still apply. In no event shall the Royal Society of Chemistry be held responsible for any errors or omissions in this *Accepted Manuscript* or any consequences arising from the use of any information it contains.

ARTICLE

Photoemission from diamond films and substrates into water: Dynamics of solvated electrons and implications for diamond photoelectrochemistry.

Cite this. DOI. 10.1039/x0xx00000x

Received 00th January 2012,
Accepted 00th January 2012

DOI. 10.1039/x0xx00000x

www.rsc.org/

R.J. Hamers,^a J.A. Bandy,^a D. Zhu,^a and L. Zhang^a

Illumination of diamond with above-bandgap light results in emission of electrons into water and formation of solvated electrons. Here we characterize the materials factors that affect that dynamics of the solvated electrons produced by illumination of niobium substrates and of diamond thin films grown on niobium substrates using transient absorption spectroscopy, and we relate the solvated electron dynamics to the ability to reduce N_2 to NH_3 . For diamond films grown on niobium substrates for different lengths of time, the initial yield of electrons is similar for the different samples, but the lifetime of the solvated electrons increases approximately 10-fold as the film grows. The time-averaged solvated electron concentration and the yield of NH_3 produced from N_2 both show maxima for films grown for 1-2 hours, with thicknesses of 100-200 nm. Measurements at different values of pH on boron-doped diamond films show that the instantaneous electron emission is nearly independent of pH, but the solvated electron lifetime becomes longer as the pH is increased from pH=2 to pH=5. Finally, we also illustrate an important caveat arising from the fact that charge neutrality requires that light-induced emission of electrons from diamond must be accompanied by corresponding oxidation reactions. In situations where the valence band holes cannot readily induce solution-phase oxidation reactions, the diamond itself can be etched by reacting with water to produce CO. Implications for other reactions such as photocatalytic CO_2 reduction are discussed, along with strategies for mitigating the potential photo-etching phenomena.

A. Introduction

Diamond is well known for its outstanding chemical and physical properties.⁽¹⁾ Included among these are a wide window of stability as a function of electrochemical potential and pH, and a very high overpotential for reduction of H^+ to H_2 .⁽¹⁾ (2) While the electrochemistry of diamond has been heavily exploited,^(1, 3-7) fewer studies have investigated its photoelectrochemistry.⁽⁸⁻¹¹⁾ One particularly important property of diamond is that its very high conduction band energy leads to negative electron affinity (NEA).⁽¹²⁻¹⁶⁾ In NEA, the conduction band lies above the free energy of a stationary electron in vacuum, often referred to as the "vacuum level". Termination of the surface with H atoms assures that the C-H surface dipole enables electron emission in a nearly barrier-free manner. ⁽¹²⁾ One consequence of negative electron affinity is that illumination of diamond with above-bandgap light leads to facile electron of emission of electrons. The emission of electrons into vacuum has been widely studied because of its potential applications such as display technologies.⁽¹⁷⁻¹⁹⁾ The emission of electrons is not limited to vacuum, and in principle NEA can lead to emission of electrons into gases and even liquids. These

environments are interesting chemically because they provide pathways toward new types of non-thermal chemistry.^(20, 21)

Recently we performed the first studies showing the ability of diamond to photo-emit electrons into water, with direct detection of solvated electrons enabled by transient absorption spectroscopy. ⁽²⁰⁾

Fig. 1 shows an energy level diagram for an H-terminated diamond surface in contact with an aqueous solution. Also depicted are some reduction reactions relevant to the diamond's unique photoemissive abilities, along with the reduction potentials at pH=7. These potentials were obtained from tabulated standard potentials^(22, 23) using the Nernst equation to calculate values at pH=7, leaving other reactants and products in their standard states. Of particular interest are diamond's ability to produce solvated electrons, atomic hydrogen, and the one-electron reduction of CO_2 to the CO_2^- anion. These reactions occur at strong negative potentials that cannot be reached by any other common semiconductor electrode conduction band. Of these reactions, the formation of solvated electrons is the first step, since other reactants (such as CO_2 or H^+) are usually

present at much lower concentrations compared with the ~55 Molar concentration of water molecules in pure water.

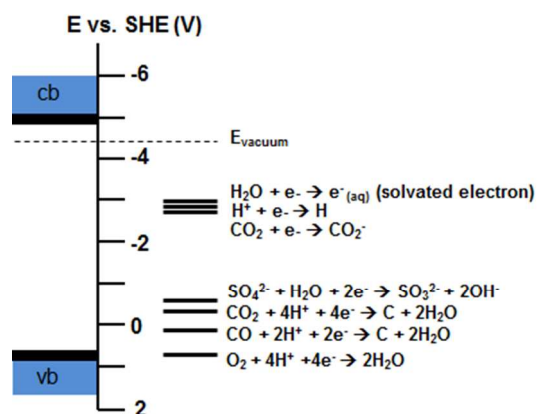


Fig. 1. H-terminated diamond in contact with aqueous electrolyte; electrochemical reduction potentials shown are for pH=7 with other reactants and products at their thermodynamic standard states. Valence band (vb) and conduction band (cb) energies are typical for H-terminated diamond.

The reactions depicted closer to the valence band are important because, as described later, photoemission of electrons must be accompanied by oxidation reactions. Fig. 1 depicts some potentially relevant reactions (written as reduction reactions, to maintain consistency with standard electrochemical literature) that can occur at the diamond surface under appropriate conditions.

Here we describe recent experiments investigating some of the properties of diamond and the adjacent electrolyte that influence the emission of electrons into water and some caveats that are important in understanding the effective use of diamond to induce new chemistry.

B. Results

B1. Solvated electrons from diamond thin films.

In previous work,^(20, 21) we demonstrated that solvated electrons could be produced in water by excitation of diamond using above-bandgap light and that smaller, but non-zero, emission could also be detected at slightly longer wavelengths. Since diamond can be easily grown on a variety of different substrates, we aimed to understand whether diamond thin films on metallic substrates would provide similar performance compared with bulk diamond samples and, if so, to what extent the electron emission would depend on the thickness of the films.

We explored the emission of electrons from diamond thin films grown on niobium. Niobium substrates are widely used as substrates for diamond films used in water purification,^(24, 25) in part because niobium is chemically robust in water. Fig. 2 illustrates the apparatus used for transient absorption measurement of solvated electrons

produced by diamond. Fig. 3 shows the change in transmission of the 705 nm beam after the sample is excited with above-bandgap light (213 nm) with data from a fresh Nb surface and also diamond thin films grown on Nb. These diamond thin films were grown via

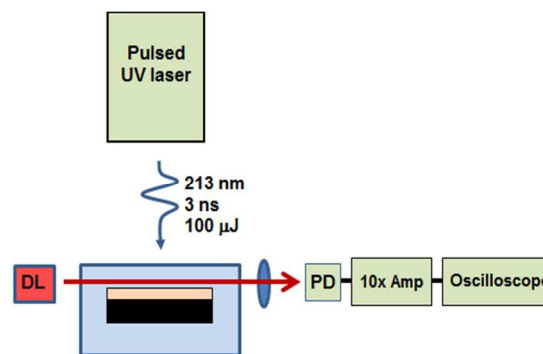


Fig. 2. Illustration of transient absorption apparatus for measuring solvated electron emission from diamond. The sample is a diamond thin film on Nb substrate, immersed in a cuvette filled with water. A fast photodiode (PD), amplifier and oscilloscope record the change in intensity of light from a 705 nm diode laser (DL) after the sample is excited by a pulsed UV laser.

microwave plasma-enhanced chemical vapour deposition for different lengths of time ranging from 10 minutes to 4 hours. In each case the diamond thin film are immersed in a solution of deionized water. The decreases in intensity at $t=0$ arise from the emission of solvated electrons, which have a broad absorption peak centered near 692 nm at room temperature.^(26, 27) Fig. 3 shows that solvated electrons are observed being emitted from both the starting Nb surface and from the diamond films on Nb substrates.

Due to the complex geometry of the 705 nm detection beam relative to the sample, the absolute amplitude of the transmitted intensity cannot be easily related to an electron concentration. However, as all samples use the same geometry, the amplitudes can be compared between different samples. The data in Fig. 3 were fitted to simple exponential functions of the form $\Delta I = A_0 \exp^{-t/\tau}$. The resulting fits are shown in Fig. 3, and the extracted values of electron lifetime τ and the maximum amplitude of the solvated electron signal A_0 are graphed in Fig. 4.

The amplitude of the initial solvated electron signal at time=0 is a direct measure of the efficiency of electron emission, while the lifetime is a measure of the available decay channels. The values graphed in Fig. 4 show that the instantaneous amplitudes (e.g., the decrease in transmission at $t=0$) are similar for the bare Nb surface and for the diamond films at all growth times, although a very small decrease in A_0 is observed (Fig. 4b) as the film thickness increases. Much more significant is that the *lifetime* of the solvated electrons increases from 77 ns on the bare Nb surface to a constant value of ~600 ns on samples grown for 2 hours or more (Fig. 4a).

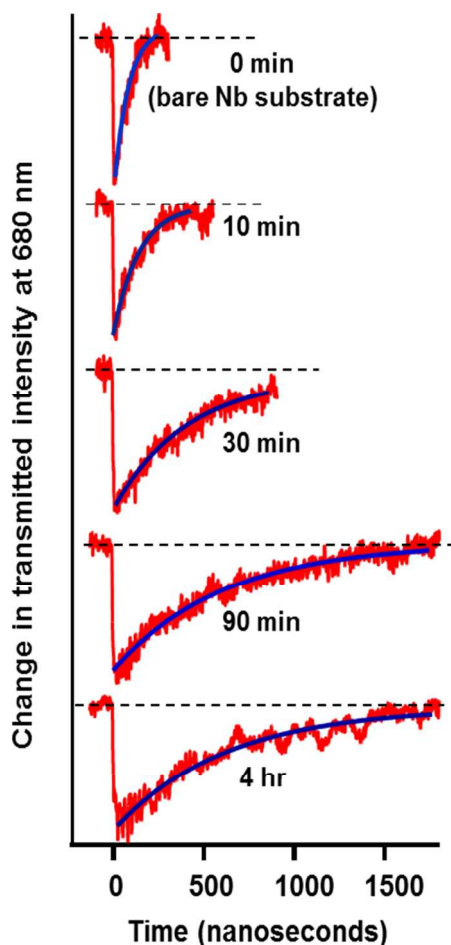


Fig. 3. Transient absorption measurements showing transient decrease in the transmission of the 705 nm laser. Measurements are shown on the starting bare Nb substrate and on diamond films grown on Nb for the indicated lengths of time up to 4 hours.

In our previous work(20, 21) we showed that solvated electrons were able to induce photocatalytic reduction of N_2 to NH_3 . This specific reaction is a stringent test of the ability to initiate new chemistry as this reaction has one of the largest known reaction barriers(28) and therefore cannot be performed efficiently with any known photocatalyst.(29) The critical step in the reaction is the formation of $N_2 + e^- + H^+ \rightarrow N_2H$, which requires approximately 3 eV of energy.(28) In photocatalytic applications, the overall yield of the reactions is expected to vary depending on the time-averaged concentrations of electrons. While electron-induced reactions, such as N_2 reduction, are complex and their overall kinetics may not be a simple function of the electron concentration, we calculated the overall area of the exponential curves in Fig. 4c using $Area = A_0\tau$, because the data are well fit by simple exponential decays. Since the maximum electron yield A_0 has a small decrease with increasing growth time, the area $Area = A_0\tau$ has a slight maximum, which occurs after a time of approximately 2 hours.

Fig. 4d shows experimental data depicting the yield of ammonia (NH_3) produced when the samples of Fig. 4 were immersed in N_2 -saturated water with 10 mM Na_2SO_4 , and illuminated continuously with light from a 450 W HgXe lamp. These catalytic yield data show that there is a clear maximum in the ammonia yield on films grown for approximately 1 hour. While the diamond film growth time that yields the maximum electron yield with pulsed excitation (~ 2 hours) is slightly different than the growth time yielding the best photocatalytic activity with continuous illumination (~ 1 hour), both appear to show best performance using films that have been grown for approximately 1-2 hours. Electron microscopy images of the films (not shown) reveal that the diamond growth is continuous within ~ 30 minutes of growth and that the film thickness after 1-2 hours of growth is approximately 100-200 nm as measured by ellipsometry.

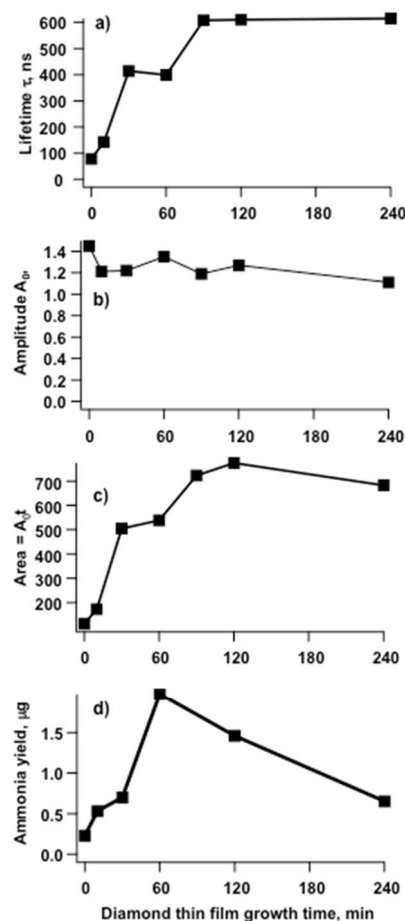


Fig. 4. Analysis of the data from Fig. 3, showing how growth time affects specific solvated electron properties and the resulting catalytic performance. 3. a) electron lifetime, b) maximum amplitude of transient, c) total area under electron decay curve, and d) ammonia yield.

We also used scanning electron microscopy to characterize the changes in the diamond film growth. Fig. 5 shows a scanning electron microscope image of the diamond film on Nb after growth for 1 hour. At this point the surface shows diamond crystallites that are approximately 50-150 nm in size. Measurements of the film thickness show an average thickness of approximately 150 nm. Since the grain size and ellipsometric thickness are nearly identical, this indicates that the film is just on the threshold of being continuous. Images at longer times show larger grain sizes and a continued evolution of the morphology.

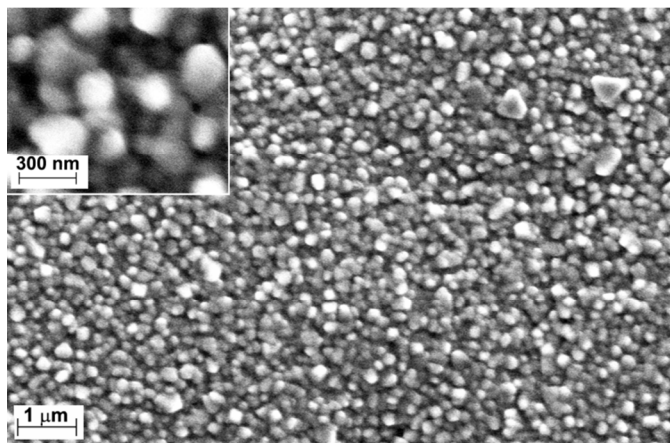


Fig. 5. Scanning electron microscope images of diamond film after growth for 1 hour. The inset shows a higher-magnification of a region from the same sample.

B2. Influence of solution pH on electron emission.

While the data in Fig. 1-4 were obtained at pH=7, the fate of solvated electrons is strongly dependent on the pH. It is well known that solvated electrons rapidly react with H^+ to form neutral atomic hydrogen atoms (H^\bullet), via $H^+ + e^- \rightarrow H^\bullet$. Hydrogen atoms are highly reactive, and in our recent computational study of N_2 reduction to NH_3 (21) we found that this reaction plays a central role in the overall catalytic reduction efficiency. To test the dependence of electron emission on pH, we conducted studies using free-standing, boron-doped diamond substrates. These substrates were chosen because they can easily be purchased and act as a great standard. (The corrosion is only an issue if you bias the substrate positively, which we do not want to really do anyway. The acid does not react at a noticeable rate, even with copper, in case you did not know.)

Fig. 6a shows transient absorption measurements of electron emission from a boron-doped diamond sample into solutions of varying pH, all measured using 213 nm excitation. In each case the pH was controlled using the NaH_2PO_4 - Na_2HPO_4 buffer (1 mM of combined concentration) for pH=5 and pH=7, and using H_3PO_4 for pH=2 and pH=3. For pH=7 and pH=5 relatively long solvated electron lifetimes of 255 and 310 nanoseconds are observed; similar results are also observed at pH=9. However, as the pH is decreased to pH=3 the solvated electron lifetime decreases to 37 ns, and for

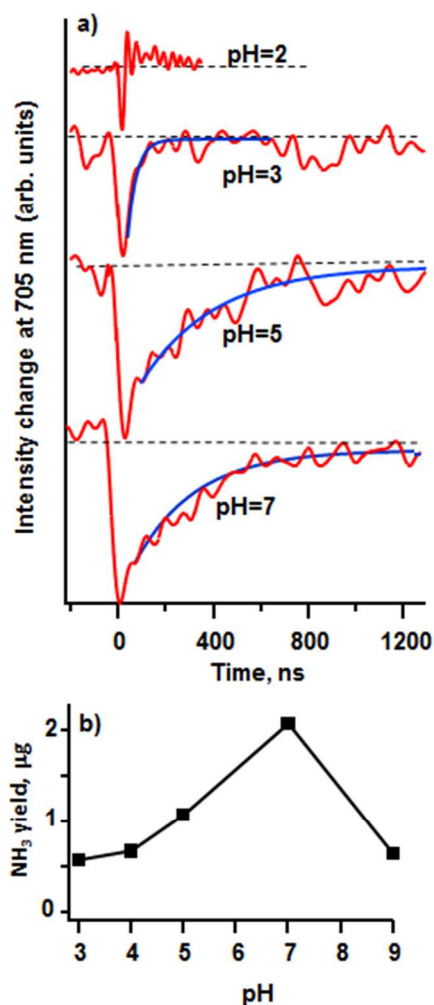


Fig. 6. Influence of pH on solvated electron dynamics and subsequent chemistry. a) Transient absorption spectra from boron-doped diamond at different values of pH. b) ammonia yield as a function of pH.

pH=2 the lifetime is <10 ns and limited by the time resolution of the detection electronics.

Fig. 6b shows the corresponding ammonia yield data as a function of pH, measured in N_2 -saturated water. The overall ammonia yield reaches a maximum near pH=7.

Our data indicate that for pH<5 the solvated electron kinetics are controlled by the reaction $H^+ + e^- \rightarrow H^\bullet$. For pH>5, the lifetimes are likely dominated by other reactions and/or possibly by recombination with the diamond substrate. The lifetimes observed with highly boron-doped diamond are slightly shorter than those observed on the diamond thin films grown on Nb. This suggests that there may be some impact of the diamond itself on the solvated electron lifetime, possibly via image-charge effects or by material-dependent recombination pathways. Computational modelling

studies of the overall N_2 to NH_3 reaction pathway show that the only feasible reaction sequence involves.

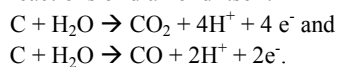
- 1) Diamond + H_2O + light $\rightarrow e^-$ (solvated electron)
- 2) e^- (aq) + $H^+ \rightarrow H\cdot$
- 3) $H\cdot$ + $N_2 \rightarrow N_2H$
- 4) N_2H + $H\cdot \rightarrow N_2H_2$.

N_2H_2 is a very stable molecule that can be rapidly reduced to NH_3 .(28) In this reaction sequence, atomic hydrogen produced by reaction of solvated electrons plays a key role in two distinct steps. While it might be expected that the highest ammonia yield would be observed at the lowest pH (where the solvated electrons react most rapidly and presumably produce the highest concentration of H), the reaction yield is actually highest at intermediate pH. Detailed rate modeling is able to reproduce this trend by including a wider range of side-reactions.(21) One reaction of particularly great importance is the bimolecular reaction $H\cdot + H\cdot \rightarrow H_2$ (gas), which becomes a particularly important alternative reaction pathway at low pH. While much remains to be learned about the reaction pathways of such high-energy species, it is clear that the ability to produce solvated electrons by photoexcitation of diamond enables chemistry to be investigated in an entirely new regime not accessible with conventional electrochemistry or other semiconductor photoelectrochemistry.

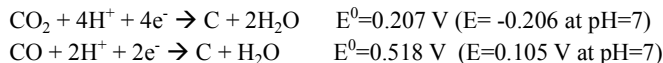
B3. Photo-induced etching of diamond. Caveats and implications for photocatalytic reduction of CO_2 .

The emission of electrons into water must always be accompanied by oxidation processes in order for the diamond to maintain charge neutrality. Consequently, when investigating diamond for catalytic reduction reactions, it is equally important to consider the oxidation reactions induced by the valence band holes.

In water, holes in diamond's valence band have several oxidation pathways. As shown in Fig. 1, for diamond samples with electron affinity of approximately -0.8 V, the 5.5 eV bandgap places the valence band approximately 4.7 eV below the vacuum level or approximately -0.26 V relative to the standard hydrogen electrode. Water oxidation at pH=0 has a standard redox reduction potential ($O_2+4H^+ +4e^- \rightarrow 2H_2O$) of 1.23 V vs. SHE, but at pH=7 the reduction potential is approximately 0.81 V vs. SHE. Thus, if the valence band lies more positive than +0.81 eV (or equivalently, more than ~5.2 V below vacuum) then it is thermodynamically capable of oxidizing water to produce $O_2 + H^+$. However, diamond and other carbon-based materials have an additional pathway, which is through oxidation of the substrate itself. Many prior studies have shown that under acidic conditions carbon can be oxidized at potentials of ~ 0.8 V to form CO_2 and CO .(30-33) There are two important oxidation reactions of diamond itself.



The reduction potentials associated with the corresponding reduction reactions are. (23, 30)



At pH=7, oxidation of carbon to form CO becomes possible for potentials more positive than 0.105 V, while oxidation to form CO_2 is possible for potentials more positive than -0.206 V (in both cases assuming gaseous products produced at 1 atmosphere pressure). In either case, at circumneutral pH, oxidation of the diamond substrate to form CO and/or CO_2 is both thermodynamically favored over oxidation of water.

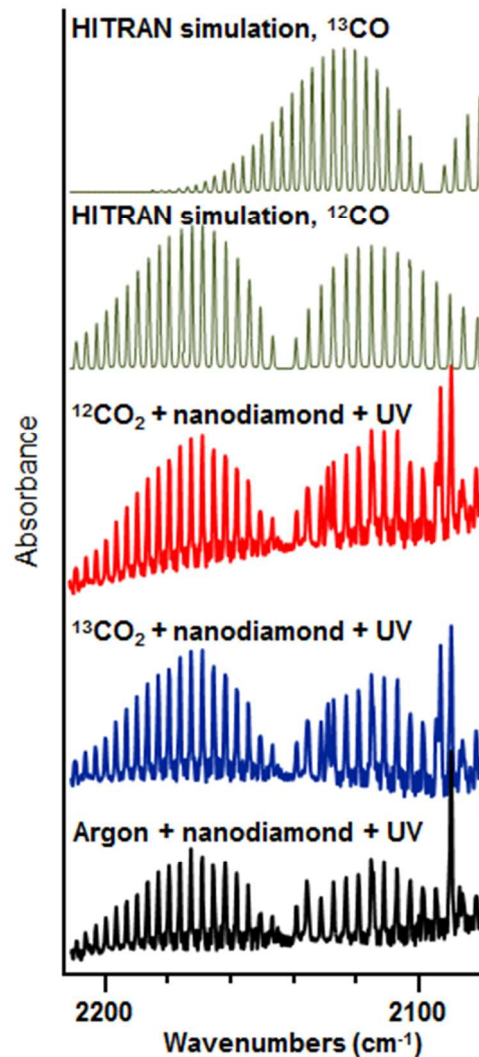


Fig. 7. Infrared measurements of CO produced from H-terminated nanodiamond illuminated in water with different dissolved gases, along with the computer simulations of spectra for ^{12}CO and ^{13}CO .

Because complex, multi-electron reactions such as the above reactions for oxidation of water and of carbon are often strongly kinetically hindered, it is difficult to predict what valence band reactions will dominate. However, a key consequence of the above thermodynamic analysis is that unless steps are taken to provide alternative pathways for the valence-band holes, photo-induced

etching of the diamond to produce CO and CO₂ as products is thermodynamically allowed. To illustrate this, we conducted experiments using H-terminated detonation nanodiamond in aqueous 0.1 M KCl solution. In these studies, nanodiamond powder was cleaned and then H-terminated by heating in H₂ at 750°C. The H-terminated powder was then stirred into an aqueous solution of 0.1 M KCl. The solutions were then sparged with argon, CO₂ or isotopically labeled ¹³CO₂ for 30 minutes and illuminated with UV light. Since natural-abundance CO₂ is ~99% ¹²CO₂, we refer to this as ¹²CO₂. After illuminating for 30 minutes, the gas-phase products were analyzed by Fourier-transform infrared spectroscopy.

Fig. 7 shows the resulting experimental spectra of the gaseous products in the primary CO absorption region, along with simulations of the expected spectra of ¹³CO and ¹²CO using the HITRAN spectral database.⁽³⁴⁾ These data show several important facts. First, ¹²CO production is observed in the solutions saturated with ¹²CO₂, ¹³CO₂, and argon. In each case, the resulting spectrum matches almost perfectly the expected spectrum of ¹²CO. Even when the solution was purged using isotopically pure ¹³CO₂, the major isotope of CO produced is ¹²CO. This isotope distribution shows that the vast majority of the CO produced does not come from the gas-phase CO₂ in the solution, but must instead come from the diamond sample itself. This conclusion is confirmed by the fact that CO is also observed when the solution is extensively purged with ultra-pure argon. In this case the only significant source of carbon in the system is the diamond powder itself.

As we will report elsewhere, the problem of photo-induced oxidation of diamond can be alleviated, but great care must always be taken to ensure that the reactions are truly catalytic. One approach is to use conductive diamond samples, and to connect the diamond to another electrode, such as Pt, that has faster oxidation-reduction kinetics. The intentional addition of species that are readily oxidized by the Pt and/or by the valence band holes can also reduce the problem. This general approach was recognized more than 50 years ago in the seminal work by Fujishima and Honda using TiO₂ to photocatalyze oxidation reaction.⁽³⁵⁾ In that work they used illuminated TiO₂ to oxidize organic species, but connected the TiO₂ to a Pt electrode to achieve reduction reactions that are otherwise very slow on TiO₂ because of its shallow conduction band energy.⁽³⁵⁾ On diamond the situation is reversed, with the electron emission being facile but corresponding oxidation reactions being sluggish and problematic.

The problem of photo-etching is most severe with nano-diamond powder, since in this case the overall low crystal quality and presence of many under-coordinated surface sites makes the surfaces more reactive. To avoid these problems, several modifications to the experimental procedures are necessary, with the goal of ensuring that the valence-band holes cannot oxidize diamond to CO or CO₂. These modifications, as explained in the experimental section, primarily involve using a Pt electrode in contact with a redox couple having facile oxidation kinetics. More detailed procedures and the enablement of selective CO₂ reduction without diamond etching will be described elsewhere.⁽³⁶⁾

C. Discussion.

While photoemission into water has some relation to photoemission into vacuum, there are also significant differences, such as the high electric field that can be present in the electrical double-layer, and the fact that electrons can be trapped near interfaces of a solid-liquid interface. Benderskii and co-workers⁽³⁷⁾ investigated photoemission from metals into liquids and noted that there are two possible mechanisms of photoemission. One, a direct surface effect that is controlled by the electric field component perpendicular to the surface, and two, a volumetric effect that is not dependent on the optical polarization. Under the conditions of our experiments (excitation directed normal to the surface) only the volumetric effect should be possible since with normal incidence there is no component of electric field perpendicular to the interface.⁽³⁷⁾

The presence of solvated electrons was inferred as early as the 1970's from steady-state photocurrent measurements of photocurrents induced in water containing various electron acceptors and illuminated with ultraviolet light.⁽³⁷⁻³⁹⁾ Yet, to the best of our knowledge the present work is the first direct measurement of solvated electrons from a metal by transient absorption spectroscopy. Our data show, somewhat surprisingly, that the major change observed in growing diamond films onto Nb is a dramatic increase in the *lifetime* of the solvated electrons. This can be understood on the basis of a simple model depicted in Fig. 8.

Metal surfaces contain a continuum of states, and therefore when an

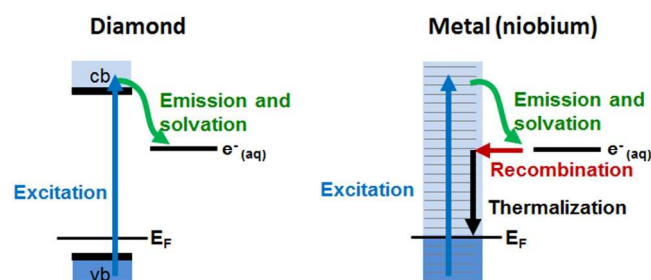


Fig. 8: Schematic depiction of processes controlling solvated electron lifetime on diamond vs. metal surfaces.

electron is injected into the solution and becomes solvated, it has a large number of degenerate states associated with the continuum of empty states of the metal. Thus, the electron can easily recombine and thermalize within the metal. In contrast, when an electron is ejected from a diamond-coated surface, the emission is essentially irreversible because the solvated electron energy is well below the conduction-band minimum. There are no (or few) electron states in diamond at the energy of the solvated electron, and therefore no possibility for the electron to recombine without simultaneously being able to lose large amounts (~ 3 eV) of energy. Thus, on metals it is likely that the lifetime is controlled by recombination in the metallic states, while in the case of a diamond-coated electrode the lifetime is controlled by chemical processes such as reduction of protons, described earlier. While much remains to be learned about the dynamics of electron emission and its implications for chemical

processes, the ability to easily create solvated electrons from a solid-state material brings with it a range of new opportunities for high-energy chemistry.

D. Experimental

Materials and methods

Growth of diamond thin films. Niobium substrates were seeded by polishing with 0-2 micron and 0-0.1 micron sized diamond particles. To remove any of the larger sized particles and aggregates, the polishing was followed by sonication in methanol followed by water. Diamond growth was accomplished using a microwave plasma-enhanced chemical vapor deposition system using a mixture of hydrogen and methane gas. Growth consisted of an initial 10 minute nucleation phase using a H₂ and CH₄ flow rates of 200 standard cubic centimeters per minute (sccm) and 2 sccm, respectively, with a microwave power of 1000 W. The nucleation phase was followed by a growth phase using a 200 sccm and 1 sccm flow rates for H₂ and methane, respectively, and a microwave power of 800 watts. In the growth phase, the substrate temperature is approximately 750 °C as measured by an optical pyrometer. Finally, the growth phase was followed by a 10 min etching in hydrogen plasma only to remove/reduce sp² hybridized carbon on the surface. In all phases, the pressure in the chamber is maintained at 48 torr.

Measurement of solvated electrons. Solvated electrons were measured using transient absorption spectroscopy. An ultraviolet pulsed laser (NT340, EKSPLA, Inc., Vilnius, Lithuania), was used to excite the samples at 213 nm, with the pulse energy adjusted to 1.5 mJ using a polarizing prism. A 705 nm diode laser (Newport LP705-SF15) with a F240FC-780 fiber collimator passed immediately in front of the sample. The transmitted light was detected using a 1.2 GHz silicon detector, Newport model 818-BB-21, amplified using FEMTO amplifier, DHPA-100 (100 V/A transimpedance, 20 MHz bandwidth) and recorded using a 4 GHz digital oscilloscope (Agilent Model DSO9404A). To reduce radio-frequency noise from the pulsed laser, a background subtraction is typically performed. After each sample is measured under the desired conditions, the solution is then acidified with H₂SO₄, which reacts rapidly with the solvated electrons but leaves all other properties unchanged; this background spectrum is recorded and subtracted from the original transient.

Measurement of ammonia yield. UV illumination used a Newport Model 6278 UV-enhanced Xenon lamp, 450 Watts electrical power. The light was passed through a water-cell to remove infrared light, and then collimated onto the sample. Ammonia yield experiments were performed in a 2-compartment cell with a separating glass frit. The sample was immersed in a solution of 10 mM Na₂SO₄; the reference electrode consisted of a Pt wire immersed in a I⁻/I₃⁻ solution with an I⁻/I₃⁻ concentration ratio of 250:1. In experiments reported here, the sample was also biased at -0.3 V relative to the reference electrode in order to minimize the possibility of the valence band holes inducing etching or other oxidation reactions. Control experiments without bias showed this small bias to have no

significant effect on ammonia yield. Ammonia yield was measured using the indophenol blue method. In this method, 0.100 ml of a 1 M NaOH solution containing 5% salicylic acid and 5% sodium citrate (by weight) was added to 2 ml of sample solution, followed by addition of 0.02 ml of 0.05 M NaClO and 0.02 ml of an aqueous solution of 1% (by weight) Na[Fe(NO)(CN)₅]. The absorption spectrum was taken with a Shimadzu 2401PC Ultraviolet-Visible Spectrophotometer after allowing the mixture to stand for 1 hour. The formation of indophenol blue was determined by reading the absorbance at a wavelength of 700 nm. Appropriate standards were run to generate a working curve for quantitative analysis.

Diamond photo-etching. Detonation nano-diamond (4-6 nm diameter) was first hydrogen-terminated at 750 °C in a tube furnace at atmospheric pressure under a 50 sccm H₂ flow for 3.5 hours. It was then dispersed in 0.1 M KCl aqueous solution (nanodiamond powder concentration. 1 g/L). 18.2 MΩ NanoPure (Barnstead) water was used to minimize any possible organic contamination. The solution was then purged with CO₂ or Argon for 30 min under ambient pressure and exposed to ultraviolet light for 16 hours with constant stirring. The reaction products were passed through a valve directly into a custom-made infrared gas cell for analysis of the gas-phase products by Fourier-transform infrared spectroscopy (Bruker Vertex 70 with a liquid nitrogen-cooled HgCdTe detector).

E. Conclusions

Our results show that the dynamics of the solvated electrons play a crucial role in the overall efficiency of photocatalytic reactions at diamond surfaces. While both metals (niobium) and diamond are able to create solvated electrons upon excitation with ultraviolet light, the electrons produced at niobium surfaces exhibit a much shorter lifetime. The much longer lifetime for electrons produced by diamond likely arises from the absence of any electronic states in the diamond bandgap that are energetically degenerate with the solvated electrons. Therefore the bandgap of diamond causes electron emission to be an *irreversible* process: once the electron is emitted, its primary pathway involves chemical reduction reactions. In contrast, on metals the presence of degenerate states leads to shorter lifetimes for the solvated electrons. The longer electron lifetimes of the solvated electrons produced at diamond surfaces provides greater opportunity for the electrons to initiate new chemistry. New high-energy reactions such as N₂ reduction and, in principle, CO₂ reduction via a simple 1-electron reduction (instead of competing proton-coupled electron transfer processes) are therefore possible.

To realize the effective utilization of diamond for photocatalysis, it is essential to also control the valence-band holes to ensure the diamond surface is not corroded. These strategies can be chemical in nature by providing sacrificial reactants and/or by using alternative materials such as Pt to carry out the oxidation reactions necessary to maintain charge neutrality.

F. Acknowledgements

Studies of diamond thin film growth, diamond photoemission into aqueous media, and the resulting solvated electron dynamics were supported by the National Science Foundation Solid State and Materials Chemistry Program, Grant DMR-1207281. Studies of diamond-based CO₂ reduction were

supported in part by the Air Force Office of Scientific Research under AFOSR Award FA9550-12-1-0063.

G. Notes and references

^a Dept. of Chemistry, University of Wisconsin-Madison, 1101 University Avenue, Madison, W 53706, USA.

1. G. M. Swain, R. Ramesham, *Anal. Chem.*, 1993, **65**, 345.
2. H. B. Martin, A. Argoitia, U. Landau, A. B. Anderson, J. C. Angus, *J. Electrochem. Soc.*, 1996, **143**, L133.
3. G. M. Swain, R. Ramesham, *Anal. Chem.*, 1993, **65**, 345.
4. A. Hartl *et al.*, *Nature Mater.*, 2004, **3**, 736.
5. J. Rubio-Retama *et al.*, *Langmuir*, 2006, **22**, 5837.
6. J. Hees *et al.*, *ACS Nano*, 2011, **5**, 3339.
7. J. Hees, R. Hoffmann, N. J. Yang, C. E. Nebel, *Chem. Europ. J.*, 2013, **19**, 11287.
8. Y. V. Pleskov, A. Y. Sakharova, M. D. Krotova, L. L. Bouilov, B. V. Spitsyn, *J. Electroanal. Chem.*, 1987, **228**, 19.
9. Y. V. Pleskov, A. Y. Sakharova, E. V. Kasatkin, V. A. Shepelin, *J. Electroanal. Chem.*, 1993, **344**, 401.
10. A. Y. Sakharova *et al.*, *Russ J Electrochem*, 1995, **31**, 169.
11. Y. V. Pleskov, A. Y. Sakharova, A. V. Churikov, V. P. Varmin, I. G. Teremetskaya, *Russ J Electrochem*, 1996, **32**, 1075.
12. F. J. Himpsel, J. A. Knapp, J. A. Vanvechten, D. E. Eastman, *Phys. Rev. B*, 1979, **20**, 624.
13. L. Diederich, O. M. Kuttel, E. Schaller, L. Schlapbach, *Surf. Sci.*, 1996, **349**, 176.
14. D. Takeuchi, H. Kato, G.S.Ri, T. Yamada, P.R. Vinod, D. Hwang, C. E. Nebel, H. Okushi, and S. Yamasaki, *Appl. Phys. Lett.*, 2005, **86**, 152103.
15. L. Diederich, O. Kuttel, P. Aebi, L. Schlapbach, *Surface Science*, 1998, **418**, 219.
16. J. Cui, J. Ristein, L. Ley, *Phys. Rev. B*, 1999, **60**, 16135.
17. W. Zhu, G. P. Kochanski, S. Jin, *Science*, 1998, **282**, 1471.
18. K. Okano, K. Hoshina, S. Koizumi, K. Nishimura, *Diamond Relat. Mater.*, 1996, **5**, 19.
19. K. Okano, S. Koizumi, S. R. P. Silva, G. A. J. Amaratunga, *Nature*, 1996, **381**, 140.
20. D. Zhu, L. H. Zhang, R. E. Ruther, R. J. Hamers, *Nature Mater.*, 2013, **12**, 836.
21. J. R. Christianson, D. Zhu, R. J. Hamers, J. R. Schmidt, *J. Phys. Chem. B*, 2014, **118**, 195.
22. H. A. Schwarz, *J. Phys. Chem.*, 1991, **95**, 6697.
23. S. M. Bratsch, *J. Phys. Chem. Ref. Data*, 1989, **18**, 1.
24. M. Fryda *et al.*, *New Diamond Frontier Carbon Technol.*, 1999, **9**, 229.
25. H. Zanin *et al.*, *J. Appl. Electrochem.*, 2013, **43**, 323.
26. F. Y. Jou, G. R. Freeman, *J. Phys. Chem.*, 1979, **83**, 2383.
27. F.-Y. Jou, G. R. Freeman, *The Journal of Physical Chem.*, 1977, **81**, 909.
28. T. Bazhenova, A. Shilov, *Coordination Chem. Reviews*, 1995, **144**, 69.
29. K. Hoshino, R. Kuchii, T. Ogawa, *Applied Catalysis B: Environmental*, 2008, **79**, 81.
30. H. S. Choo *et al.*, *Journal of the Electrochemical Society*, 2007, **154**, B1017.
31. K. G. Gallagher, G. Yushin, T. F. Fuller, *Journal of the Electrochemical Society*, 2010, **157**, B820.
32. H. S. Choo *et al.*, *Journal of Power Sources*, 2008, **185**, 740.
33. J. O. Besenhard, H. P. Fritz, *Angew. Chem. Int. Ed.*, 1983, **22**, 950.
34. L. S. Rothman *et al.*, *J. Quant. Spectrosc. Radiat. Transf.*, 2010, **111**, 1568.
35. A. Fujishima, K. Honda, *Nature*, 1972, **238**, 37.
36. L. H. Zhang, R. J. Hamers, manuscript in preparation.
37. V. Benderskii, S. D. Babenko, Y. M. Zolotovskii, A. G. Krivenko, T. S. Rudenko, *J. Electroanal. Chem.*, 1974, **56**, 325.
38. A. V. Benderskii, V. A. Benderskii, A. G. Krivenko, *J. Electroanal. Chem.*, 1995, **380**, 7.
39. S. D. Babenko, V. A. Benderskii, Y. M. Zolotovskii, A. G. Krivenko, *J. Electroanal. Chem.*, 1977, **76**, 347.